Operación remota del microscopio electrónico de transmisión jeol jem-2200f

$Al_2O_{3(w)}$–$Al_2O_{3(n)}$–ZrO_2 $(TZ\text{-}3Y)_n$ multi-scale nanocomposite: An alternative for different dental applications?

A. Nevarez-Rascon, A. Aguilar-Elguezabal, E. Orrantia, M.H. Bocanegra-Bernal.

Abstract

The influence of the addition of Al_2O_3 whiskers (2.5 wt.% up to 30 wt.%) on Vickers hardness and fracture toughness in an $Al_2O_{3(n)}$+ZrO_2(TZ-3Y)$_n$ (90, 80 and 70 wt.%) composite was investigated. Green compacts were obtained by uniaxial pressing at 50 MPa and pressureless sintering at 1500 ºC in air for 2 h. After sintering, relative densities ranging from 75% to 97% were reached. The whiskers resisted particle rearrangement owing to the extensive sliding distances along the whisker boundaries during sintering and the high length/diameter ratios. Sintering becomes more difficult with increasing whisker content, because whiskers come into contact with each other, forming a rigid network which hinders densification. The 2.5 wt.% Al_2O_3 whiskers + 27.5 wt.% Al_2O_3 nanoparticles + 70 wt.% TZ-3Y composite showed a hardness > 13 GPa and a maximum fracture toughness of 6.9 MPa $m^{-1/2}$, with an average grain size of 0.4 ± 0.17 $_1$m. The observed crack deflection was an important mechanism in the improved fracture toughness of the composite. In addition, the grain size and residual porosity also seem to be factors in obtaining a wide range of

hardness as well as fracture toughness by varying the Al_2O_3 whiskers and ZrO_2 (TZ-3Y) content. The use of alumina-whisker-reinforced composites in dental applications could be promising for increasing hardness and fracture toughness compared with other materials. The reported values for these composites can compete with those of commercially available materials in different dental applications.

The development of technologies for the manufacture of new dental materials has been motivated by the demand for materials capable of supporting new specifications and applications [1]. Great progress in dental restoration techniques has been made since the 1970s through the use of ceramic materials. In some field applications, the tendency has been the substitution of the metallic substructure, including implant restoration, with ceramic materials. Esthetic quality, biocompatibility and chemical resistance are some advantages of these ceramic materials. In this context, the development of advanced dental material technologies has recently led to the application of alumina, zirconia or a combination of these [2,3]. During recent decades, a lot of research work has focused on the improvement in properties resulting from the combination of Al_2O_3 and ZrO_2 [4].

The demand for structural ceramics has led to increased interest in the processing and characterization of fiber-reinforced ceramic composite systems [5]. The majority of work concerned with the fiber reinforcement of glasses and glass–ceramics has focused on using SiC or carbon fibers. However, it is well known that the fracture toughness of ceramic materials is strongly dependent on their

microstructure. Indeed, in order to improve the fracture resistance of ceramic materials, there have been extensive studies on the incorporation of strong ceramic whiskers into ceramic matrices to form a whisker-reinforced ceramic matrix composite [6–8]. The ceramic whiskers are single crystals possessing a high degree of structural perfection and, hence, superior strength and toughness. For example, the tensile strength of ceramic silicon nitride whiskers is~50 GPa, compared with~3 GPa for glass fibers and 0.1 GPa for bulk glass [9–12]. In addition, the shape of the whiskers is generally acicular or needle-like, discontinuous, 0.1–5 lm in diameter and >5 lm long, with the potential benefit of bridging matrix microcracks and preventing them from propagating [9,13]. Xu et al. [14] found that ceramic whisker reinforcement imparted a nearly twofold increase in the flexural strength and fracture toughness of dental resin composites.

Studies conducted earlier showed that incorporating 20 vol. % of very strong microscopic SiC whiskers into a fine-grained (<2 lm) polycrystalline alumina matrix can result in a threefold increase in fracture resistance [15, 16]. This is achieved using SiC whiskers, which themselves have a fracture toughness of only~3 MPa m-1/2, a value that is comparable with that of fine-grained alumina. The strength of the whiskers and fibers can also be increased when their diameters are reduced. The addition of dispersed ZrO_2 should allow an increase in toughness by the initiation of martensitic transformation of tetragonal ZrO_2 and/or microcracking [17,18]. It has been shown that the fracture toughness of mullite 20 vol.% SiC whiskers composites, in which 20 vol.% of ZrO_2 particles are dispersed, increases substantially compared with the composite without whiskers [19]. For

example, the toughness values are 2 MPa $m^{-1/2}$, 4.7 MPa $m^{-1/2}$ and 7.7 MPa $m^{-1/2}$ for mullite, mullite + 20 vol.% SiC whiskers, mullite + 20 vol.% SiC whiskers + 20 vol.% monoclinic ZrO_2 particles, respectively. Here, microcrack toughening acts as an additional factor in whisker reinforcement. The amount of research and number of publications concerning the potential of whisker toughening has been increasing significantly. Although there have been partial overviews of these studies [15], no detailed review has yet been published on whisker toughening ceramics (WTC) in dental ceramics. Experimental studies and models based on fracture mechanics concepts indicate that five toughening mechanisms may operate in WTC. These mechanisms are crack deflection [20–22], crack bowing [21], microcracking [23], whisker pullout [24] and crack bridging by whiskers [25]. Crack bridging occurs by frictional interlocking of opposing fracture surfaces and by the formation of ligamentary bridges between them. Such phenomena have been observed in various composites such as rubber-toughened polymers [26], ceramic–metal composites [27] and coarse-grained alumina [28]. Whiskers or fibers can act as crack bridging sites like coarse grains. However, whisker loadings are limited where high sintered densities can be achieved.

High densities with high whisker loadings can be obtained by means of hot-pressing (HP) and hot isostatic pressing (HIP).

The trend today is to develop alumina–zirconia composites as an alternative to monolithic zirconia and alumina, which has been characterized by its high wear resistance, though it shows low resistance to fracture [3,29]. In the

ZrO_2–Al_2O_3 system, two composite materials can be prepared as follows: ZrO_2 reinforced with alumina particles and denoted by ATZ, or Al_2O_3 reinforced with zirconia particles, ZTA. In both cases, the fracture toughness of the ceramic matrix material is increased [30–32]. The interest of dentists, dental technicians and patients is to acquire stronger and tougher ceramic materials [33], since clinical failure of ceramic restorations is very often associated with their brittleness and low fracture toughness. Thus the improvement of the in-service reliability of a material can be achieved by increasing its fracture toughness [34]. Yttrium oxide partially stabilized zirconia (Y-TZP) ceramic is now available to dentistry through the use of computer-aided design/computer-aided manufacturing (CAD/CAM) techniques which, compared with other dental ceramics, has better mechanical performance and superior strength and fracture resistance [35–37].

The types of zirconia recently introduced to the market are commercialized for dental rehabilitation such as veneers, inlay, crowns, onlay (VINCRON) and in fixed partial dentures. These materials contain such different types of composites as yttriumdoped cation (3Y-TZP) or magnesia-doped cation (Mg-PSZ), zirconia toughened alumina (ZTA) or a combination of 3Y TZP + Mg-PSZ. It is important to note that some of the mechanical properties in these composites depend directly on the grain size. When the grain size is >1 μm, the composite behaves unstably and is susceptible to spontaneous transformation whereas, when the grain size is < 0.5 μm, a sluggish $t \rightarrow m$ transformation occurs.

With grain sizes <0.2 lm the *t → m transformation* is unlikely to happen, therefore reducing the possibility of cracking [38–40]. Whiskers were recently used to reinforce dental composites to extend their use to large stress-bearing restorations. Taking into account that zirconia or/and zirconia-based composites are interesting multifunctional materials for many further applications [41], and in spite of the different studies published by several investigators on alumina–zirconia ceramics reinforced with silicon carbide whiskers, to the authors' knowledge, studies concerning alumina–zirconia with the addition of Al_2O_3 whiskers for different dental applications has not yet been reported. Based on these expectations, the main objective of this paper is to combine the transformation toughening in ZrO_2 ceramics with the addition of different percentages of alumina whiskers in an attempt to improve the fracture toughness and hardness in alumina toughened zirconia (ATZ) ceramic composites obtained by pressureless thermal treatment at 1500 ºC for 2 h in air, and thus obtain an efficient alternative to commercial dental ceramics.

Materials and methods

Mixture preparation

High-purity α-Al_2O_3 (Baikalox SM8, Baikowski, USA; 100% α, purity >99.99%), MgO (500A, UBE Chemical Industries, Japan; purity >99.999%), and ZrO_2 + 3 mol.% Y_2O_3 (thereafter abbreviated to TZ-3Y, Tosoh, Japan; purity >99.99%) powders and Al_2O_3 whiskers (2–4x2800 nm, Aldrich, USA) were used as starting materials. Their characteristics (particle size, surface

area and theoretical density) are presented in Table 1. Homogeneous mixtures of 3 mol. % yttria-stabilized zirconia (TZ-3Y) with 10, 20 and 30 wt.% Al_2O_3 (Al_2O_3 whiskers + Al_2O_3 nanoparticles) were prepared. Al_2O_3 whiskers ranging from 2.5 to 30 wt. % were first dispersed in 500 mL ethanol with ultrasonic agitation for 30 min to destroy the agglomeration state, and the nanopowders were subsequently intensely mixed with the dispersed Al_2O_3 whiskers by stirring with a magnetic stir bar until most of ethanol had evaporated, and then the mixture was dried at 100 ºC for 12 h. To avoid any variations that can occur due to relative humidity changes, all experiments were done at the same time. In all compositions, the Al_2O_3 powder was previously doped with 25 ppm MgO powder in order to inhibit the grain growth during sintering.

Compaction and sintering

About 2.5 g of the mixture was uniaxially pressed at 50 MPa into a disk (steel die) 16 mm in diameter and 7 mm high using an Elvec Hydraulic Press at a constant strain rate of 30 kf s^{-1}. Green samples were placed into an alumina crucible with ZrO_2 + Al_2O_3 bed powders and sintered at 1500 ºC for 2 h in air at a heating rate of 10 ºC m^{-1}. After sintering, the furnace was shut off and allowed to cool down. The sintered density was measured using a geometric method with three samples per each composition. For this purpose, the thickness and diameter were measured using a digital vernier, accurate to 0.001 mm, and the weight was measured using a scale accurate to 0.1 mg, and then the average

relative density was calculated. The samples were ground and polished through

Table 1
Characteristics of commercial starting powders.

Powder	Primary particle size (μm)	BET surface area ($m^2\ g^{-1}$)	Theoretical density ($g\ cm^{-3}$)
Baikalox SM8 Al_2O_3[a]	0.050	10.0	3.98
3 mol% Y_2O_3–ZrO_2 (TZ-3Y TOSOH)[b]	0.075	17.2	6.05
MgO 500A[c]	0.053	31.9	3.58
Al_2O_3 whiskers Ø 2–4 nm, length 2800 nm[d]		125	4.00

[a] Supplied by Baikowski (USA).
[b] Supplied by TOSOH (Japan).
[c] Supplied by UBE Chemical Industries (Japan).
[d] Supplied by Sigma–Aldrich (USA).

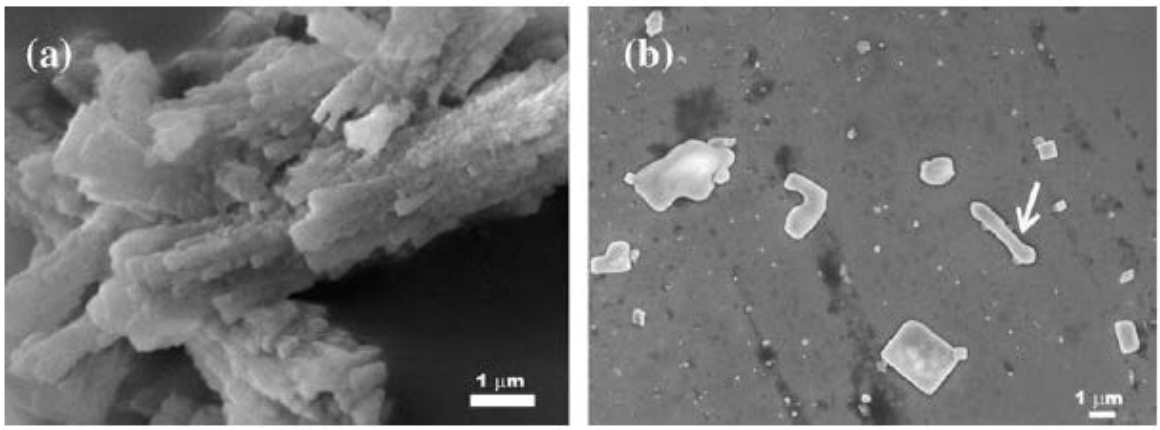

Fig. 1. SEM micrographs showing the appearance of the Al_2O_3 whiskers: (a) agglomerates of the "as received" whiskers; (b) higher magnification of dispersed whiskers showing Al_2O_3 particulates (arrow explained in the text).

SiC paper in a sequence of #400, #800 and #1200, and then polished by both 0.5 and 0.25 m diamond pastes and subsequently thermally etched in air for 40–60 min at temperatures 150 ºC below the sintering temperature. A drop of the above-dispersed Al_2O_3 whiskers was deposited onto a copper sheet.

Sample characterization

The polished and fracture surfaces as well as the Al_2O_3 whiskers were characterized by scanning electron microscopy (SEM: JEOL JSM 5800 LV, Japan, and FEG SEM: JEOL JMS 7000F, Tokyo, Japan) using an accelerating voltage of 2–10 kV after carbon coating to avoid charging during exposure to the electron beam. The average grain size of Al_2O_3 and TZ-3Y in the sintered composite was measured by the linear intercept technique using 300–400 grains for each sample.

Hardness and fracture toughness

Vickers hardness measurements were carried out on sintered samples using a Microhardness Tester FM-7. Radial-median and Palmqvist crack systems exist in material as a consequence of indentation according to Ponton and Rawlings [42]. In the present study, the cracks appear on polished surfaces for a load of 1 kg held for 10 s. For the ratio of crack length to indentation length (*c/a*) <2.3, the cracks developed were Palmqvist cracks. For a ratio >2.5, the cracks formed during indentation take the form of median cracks. A lower indentation load was used to avoid cracking or spalling around the Vickers impression, which can affect the hardness and fracture toughness measurements owing to excessive

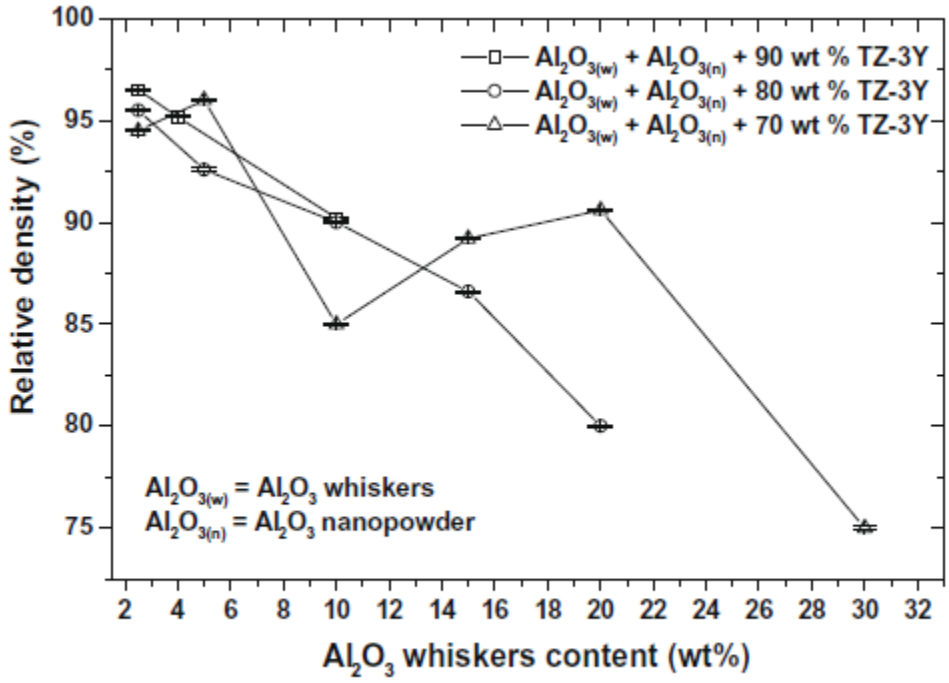

Fig. 2. Variations in relative densities as a function of Al_2O_3 whiskers content.

damage at the indentation tip or sides. Three samples per composition (diameter 12 mm, thickness 5 mm) and~20–30 indents per each measurement were made, and the average hardness was determined. The separation between neighboring indentations was more than four diagonal lengths of indentation impression according to the standard ASTM C1327-99 for Vickers indentation hardness of advanced ceramics [43]. With the help of an Olympus PMG3 optical microscope, the corresponding indentations sizes and crack lengths were measured soon after indentation in order to prevent the slow crack growth associated with the stress field which acts after removal of the indenter and with environmental effect. The indentation fracture toughness (K_{IC}) was derived from average crack length and applying the following formula [44]:

$$K_{IC} = 0.0752P/C^{3/2} \quad (1)$$

where K_{IC} is the fracture toughness, P the load, and C the crack length.

Results

In Fig. 1a, SEM reveals agglomerates of the ‘‘as received” αAl_2O_3 whiskers exhibiting lengths up to~μ5 1m with aspect ratio of 35. A combination of elongated whiskers and Al_2O_3 in the form of particulate with sizes ranging from 0.1 to 0.8μm was observed (see Fig. 1b). Some of the Al_2O_3 whiskers had diameters varying along their lengths (arrow in Fig. 1b).

The relative densities of specimens as a function of the Al_2O_3 whisker content are shown in Fig. 2. It is observed that the addition of whiskers up to~5 wt.% had no significant influence on the densification, even though the relative density decreased with an increase in Al_2O_3 whiskers. At higher whisker content, the sintered density decreased significantly in the three compositions studied, suggesting the formation of agglomerates at high Al_2O_3 whisker content.

Fig. 3a–c shows representative SEM micrographs of polished and thermally etched Al_2O_3 (2.5 wt.% Al_2O_3 whiskers + Al_2O_3 nanoparticles) + 70, 80 and 90 wt.% TZ-3Y, corresponding to samples with maximum sintered density. This figure clearly shows that all samples were crack free, with approximately the same measured average grain size and Al_2O_3 grains (darker phase) homogeneously distributed in fine TZ-3Y matrix grains (the brighter phase). The absence of whiskers or their agglomerates on the polished surface is worth noting. Examination of the sintered surfaces shows that the grain size of alumina in the composite 2.5 wt.% Al_2O_3 whiskers + 27.5 wt.% Al_2O_3 nanoparticles + 70

wt.% TZ-3Y increased (measured value of 0.48 ± 0.19μm), while the measured grain size for pure TZ-3Y decreased up to 0.32 ± 0.14μm. However, the average obtained grain size of the composite was 0.4 ± 0.17μm.

It is well known that the whiskers are normally received from commercial sources in the agglomerate state. If the whiskers

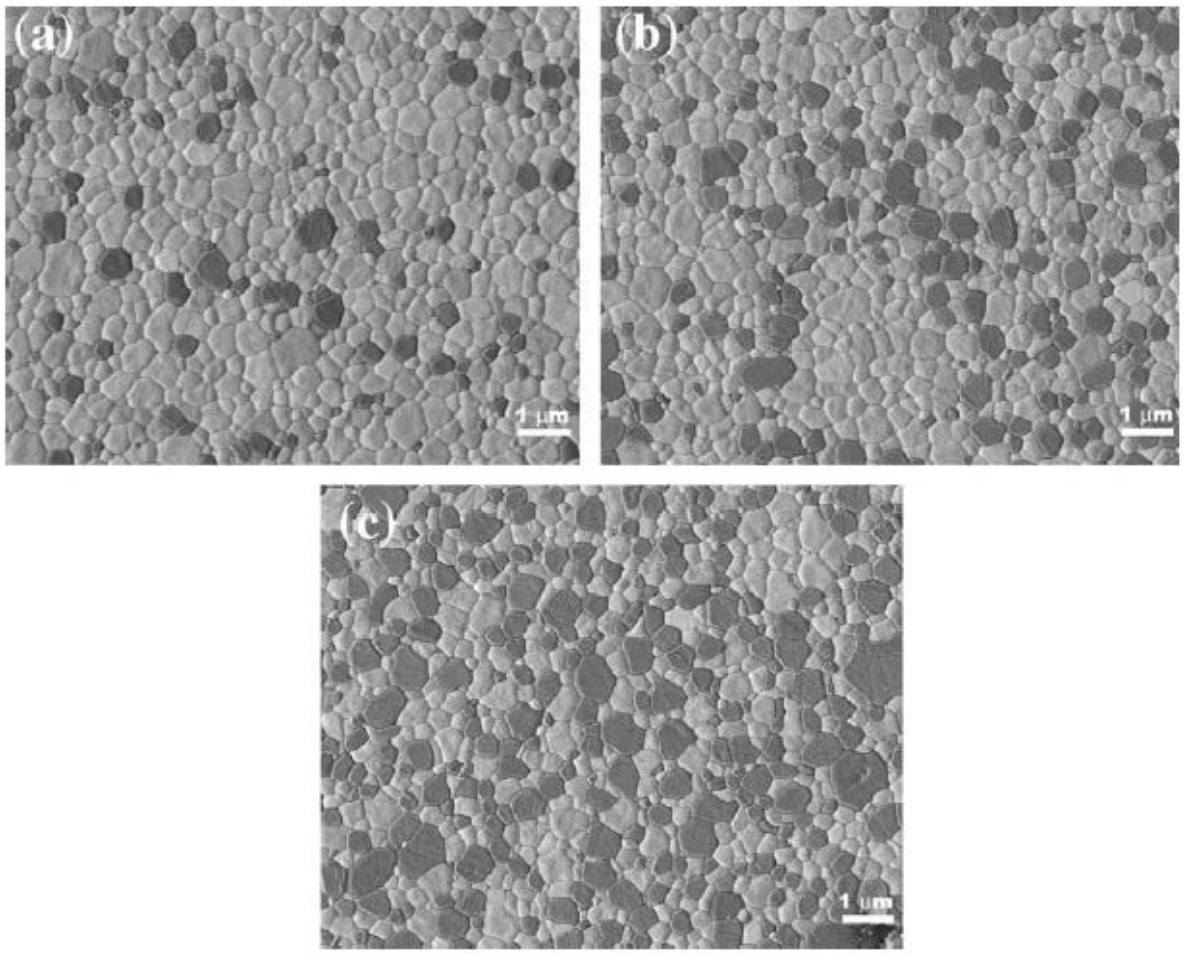

Fig. 3. SEM micrographs of polished and thermally etched samples: (a) 10 wt.% Al_2O_3 (2.5 wt.% Al_2O_3 whiskers + 7.5 wt.% Al_2O_3 nanoparticles) + 90 wt.% TZ-3Y; (b) 20 wt.%Al_2O_3 (2.5 wt.% Al_2O_3 whiskers + 17.5 wt.% Al_2O_3 nanoparticles) + 80 wt.% TZ-3Y; and (c) 30 wt.% Al_2O_3 (2.5 wt.% Al_2O_3 whiskers + 27.5 wt.% Al_2O_3 nanoparticles) + 70 wt.% TZ-3Y.

remain in that state, they remain as low density regions in the final composite, degrading the final mechanical properties and hindering grain growth. Fig. 4a–c shows this behavior, where the Al_2O_3 whisker agglomerates are

marked by a circle. At higher magnification (Fig. 4d–f), the whisker agglomerates showed morphology similar to that exposed in Fig. 1b.

Al_2O_3 whisker loadings were found to affect Vickers hardness, as shown in Fig. 5. It is observed that the hardness values show an increase with decreasing addition of Al_2O_3 whiskers. At whisker loadings below 4 wt.%, the hardness achieved by ATZ 90, 80 and 70 wt.% TZ-3Y composite was slightly superior. Meanwhile, above this percentage of whisker addition, a dramatic decrease in hardness is clearly observed. However, fracture toughness as a function of Al_2O_3 whiskers content is illustrated in Fig. 6. A similar trend to that obtained in the hardness plot (Fig. 5) is observed. Above 2.5 wt.% whisker addition, a decrease in fracture toughness occurs. However, at Al_2O_3 whisker content above ~15 wt.%, the attainable fracture toughness decreases significantly.

Discussion

Considering the mechanical properties of commercial ceramic materials, whisker-reinforced ceramic composites are materials with relatively high fracture toughness [45]. Taking into account the high fracture toughness of tetragonal zirconia polycrystal (TZP) matrix, an alternative way to improve its mechanical properties is by adding strong Al_2O_3 whiskers. As shown in Fig. 1, the ‘‘as received” alumina whiskers are free of pores and agglomerated. As mentioned above, if the whiskers remain in the agglomerate state during processing, these will remain in the final composite as low density regions, which is reflected in a low sintered density, as observed in Fig. 2, and fracture surfaces illustrated in Fig. 4d–f. Several problems are faced in obtaining adequate green composites

of WTC, one of which is their agglomeration. Whiskers tend to form large lumps during handling, and their homogeneous incorporation into the matrix powder is difficult [46], thus decreasing the packing efficiency of the composite.

The presence of whiskers in a powder compact makes sintering of the composite difficult, inasmuch as they resist particle rearrangement as a consequence of extensive sliding distances along whisker boundaries during sintering as well as high whisker aspect ratios, or ratios above a critical volume fraction. In this context, sintering becomes more difficult, increasing the whisker content, because they come into contact with each other and tend to form a rigid network. Therefore, the forces necessary to overcome the network are greater than the driving forces required for the sintering process. This behavior is reflected in Fig. 2 for whisker content >5 wt.%, where the sintered density decreased significantly in the three compositions studied, suggesting the formation of agglomerates at high Al_2O_3 whisker content, and therefore the whisker clusters can act as rigid inclusions, avoiding complete sintering and causing inhomogeneity in the phase distribution. Similar observations have been reported by Yang and Stevens [47], where large matrix particles situated at the intersection of whiskers welded the network firmly, which left interparticle porosity. Although fine particles inside the network can densify locally, the overall shrinkage is not affected by this, and consolidation slows down.

When high sintered densities must be achieved by conventional techniques (for example pressureless sintering), the whisker loading is very limited. Notwithstanding, the pressure-assisted techniques including HP and HIP

produce high densities at high whisker loadings [48] in WTA composites, with full density by HIP at 1550 ºC and 200 MPa for 1 h, where a fine-grained composite was obtained by the process.

The hardness of ceramic composites can be affected by the intrinsic deformability of the ceramic and the microstructural parameters such as present phases, grain size and orientation, residual porosity and boundary constitution [49]. The reinforcement role of the Al_2O_3 whiskers in zirconia composite might affect the increase in hardness. Above 4 wt.% of whisker addition, a dramatic decrease in hardness is clearly observed (Fig. 5). This behavior could be attributed to the difficult in dispersing Al_2O_3 whiskers homogeneously in the composite, as well as the poor cohesion between alumina whiskers and the matrix [50]. The decrease in hardness can also be attributed to the sensitivity of hardness to the de-crease in the sintered density (Fig. 2) as well as the existence of de-fects, as shown in Fig. 4a–f. In this context, the hardness value dispersion obtained in the compositions (Fig. 5) is related to the different porosity remaining in each sample. A decrease in the porosity percentage leads to an improvement in hardness.

In the literature, the hardness and the fracture toughness values of ceramics are frequently reported as a function of the grain size.

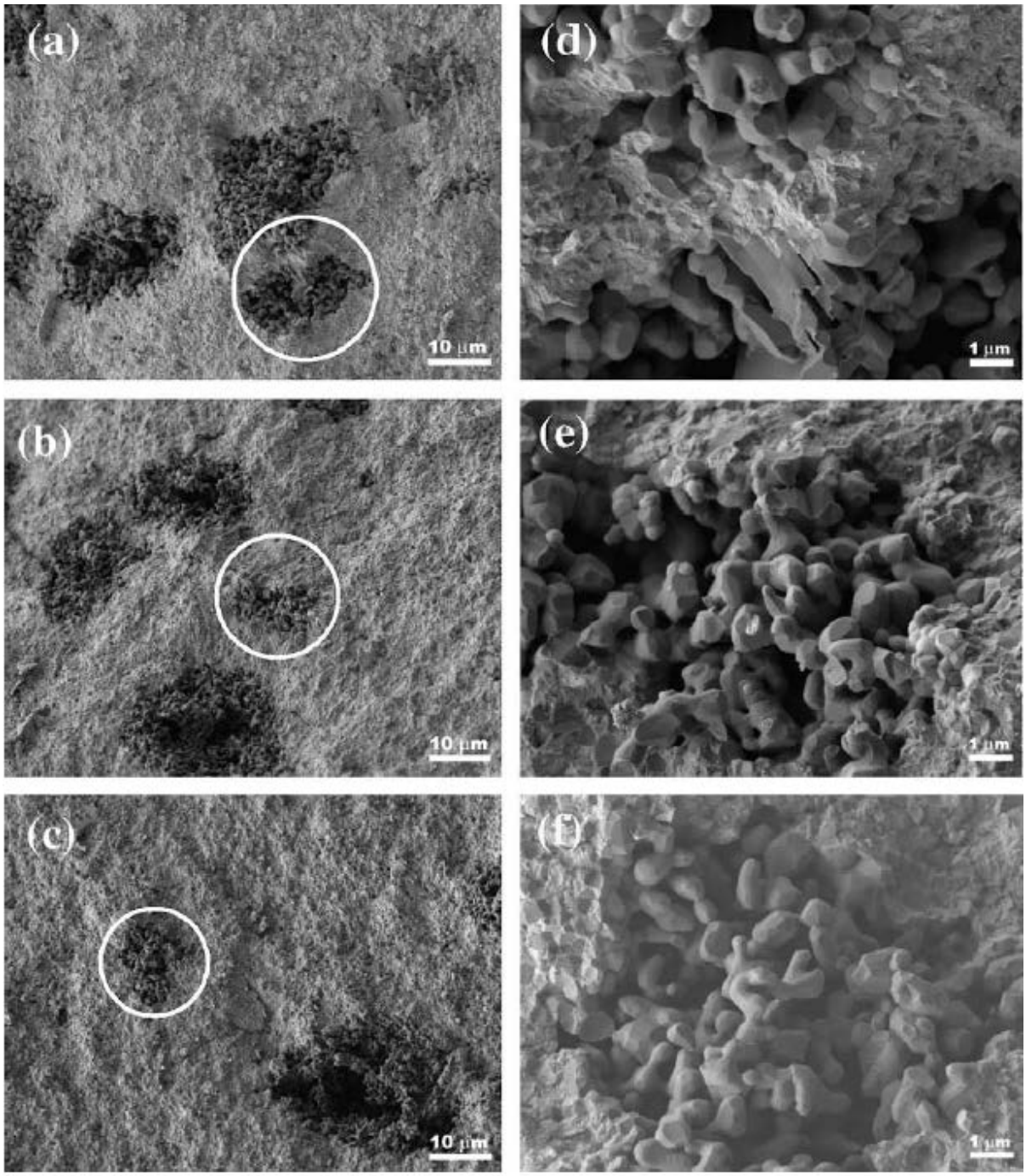

Fig. 4. SEM micrographs of fracture surfaces of pressureless sintered composites: (a) 10 wt.% Al_2O_3 (2.5 wt.% Al_2O_3 whiskers + 7.5 wt.% Al_2O_3 nanoparticles) + 90 wt.% TZ-3Y;(b) 20 wt.% Al_2O_3 (2.5 wt.% Al_2O_3 whiskers + 17.5 wt.% Al_2O_3 nanoparticles) + 80 wt.% TZ-3Y; (c) 30 wt.% Al_2O_3 (2.5 wt.% Al_2O_3 whiskers + 27.5 wt.% Al_2O_3 nanoparti-cles) + 70 wt.% TZ-3Y. (d–f) Corresponds to higher magnification of Al_2O_3 whisker agglomerates marked in white circle in (a–c).

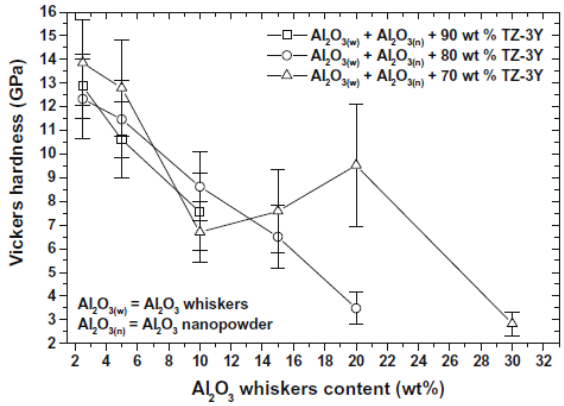

Fig. 5. Vickers hardness of ATZ nanocomposite as a function of Al_2O_3 whisker loadings.

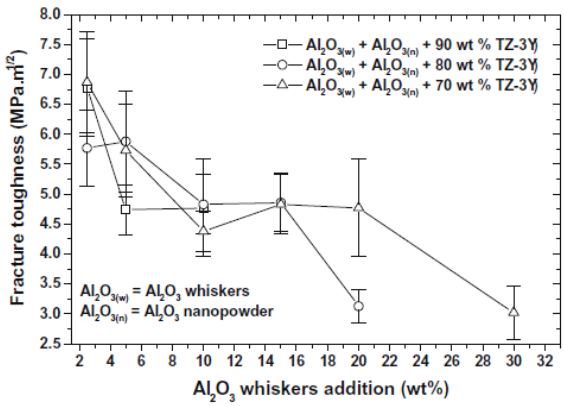

Fig. 6. Fracture toughness of ATZ nanocomposite as a function of Al_2O_3 whisker loadings.

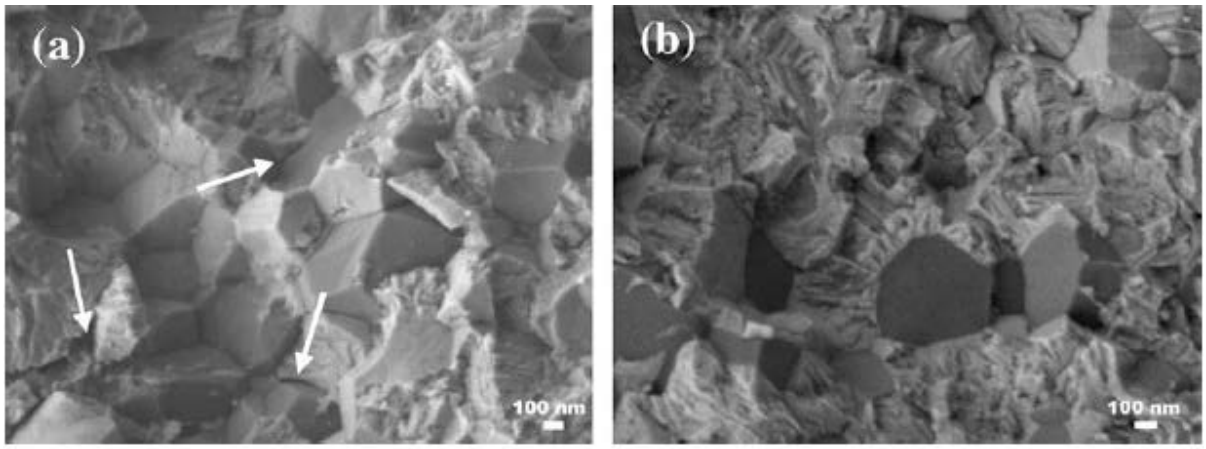

Fig. 7. Fracture surfaces of pressureless sintered composites: (a) 30 wt.% Al_2O_3 (2.5 wt.% Al_2O_3 whiskers + 27.5 wt.% Al_2O_3 nanoparticles) + 70 wt.% TZ-3Y; and (b) 30 wt.%Al_2O_3 + 70 wt.% TZ-3Y. Arrows in (a) indicate microcraks.

For example, Daguano et al. [1] reported a reduction in hardness in sintered ZrO_2–Al_2O_3 attributed to an increase in the grain size; Suzuki et al. [51] reported that Vickers hardness is correlated with porosity in the former sintering stage, while in the latter sintering stage it is correlated with grain size; and Chakravarty et al. [52] revealed improved hardness values with small grain size. In the present work, hardness > 13 GPa, which is higher than the 12 GPa of conventional Y-TZP [53], was obtained in the 30 wt.% Al_2O_3 (2.5 wt.% Al_2O_3 whiskers + 27.5 wt.% Al_2O_3 nanoparticles) + 70 wt.% TZ-3Y composition. The

measured average grain size of 0.40 ± 0.17μm for the 70 wt.% TZ-3Y composite was <1.27 ± 0.5 and 0.57 ± 0.1 1m obtained in as-sintered alumina and zirconia monoliths. Indeed, the addition of a relatively low amount of Al_2O_3 particles and whiskers in TZ-3Y seems to be enough to allow a refinement in microstructure, increasing the hardness as well as the fracture toughness. This behavior can be supported by the results of Chakravarty et al. [52] and Daguano et al. [1].

Fig. 6 is a plot showing the fracture toughness as a function of alumina whisker content. It is believed that the high fracture toughness (6.9 ± 0.9 MPa $m^{-1/2}$) value obtained in the 30 wt.% Al_2O_3 (2.5 wt.% Al_2O_3 whiskers + 27.5 wt.% Al_2O_3 nanoparticles) + 70 wt.% TZ-3Y composition can be attributed to the fracture mode, which was mainly intergranular (many pits present on the fracture surface) accompanied by a partial transgranular fracture mode, as observed in Fig. 7a, where the roughness of the fracture surface increased in comparison with the relatively smooth fracture surface shown in Fig. 7b, corresponding to the composite without Al_2O_3 whiskers content (fracture toughness of 5.4 ± 1.8 MPa $m^{-1/2}$). The mixed fracture mode results in greater fracture energy, which leads to greater fracture toughness. Similarly, it is worth noting that the intergranular fracture mode will improve the fracture toughness

The presence of microcracking in the composite (arrow marks in Fig. 7a) could contribute to the deflection of cracks and to the dispersion of its energy, therefore increasing the fracture toughness [33,54]. It is evident that the

improvement in fracture toughness is connected mainly to the presence of high deviation angles as a consequence of the tortuosity of the crack path (increase in crack deflection). Conversely, the decrease in fracture toughness in the composite free from Al_2O_3 whiskers (Fig. 7b) can be explained by the decrease in the number of crack deviations as well as deflection angles, indicating that the crack deflection mechanism is less effective in the toughening process [55].

In the behavior of the composite with and without the addition of alumina whiskers, it is evident that, comparing the whiskers versus only equiaxed particles, the geometry of these reinforcing phases is very important, inasmuch as an advancing crack necessarily finds it more difficult to avoid an intact relatively long 1-μm-diameter whisker than a 1μm-diameter grain. As a result of this, the crack is deflected around the whisker, resulting in toughening due to the additional work required in propagating a deflected crack [6,45]. In other words, in the proximity of a whisker, the propagation energy of the advancing crack can be dissipated, and the crack can be deflected or pinned. Therefore, depending on whether the advancing crack interacts with a porous or dense whisker, for the same composite the fracture toughness can range from a small value to a larger value, resulting in a scatter in the data. It is also highly probable that different fracture toughness values will be obtained in the same sample, depending on the orientation of the Al_2O_3 whiskers.

The phase transformation has generally been known to be an important contribution to the improvement in fracture toughness

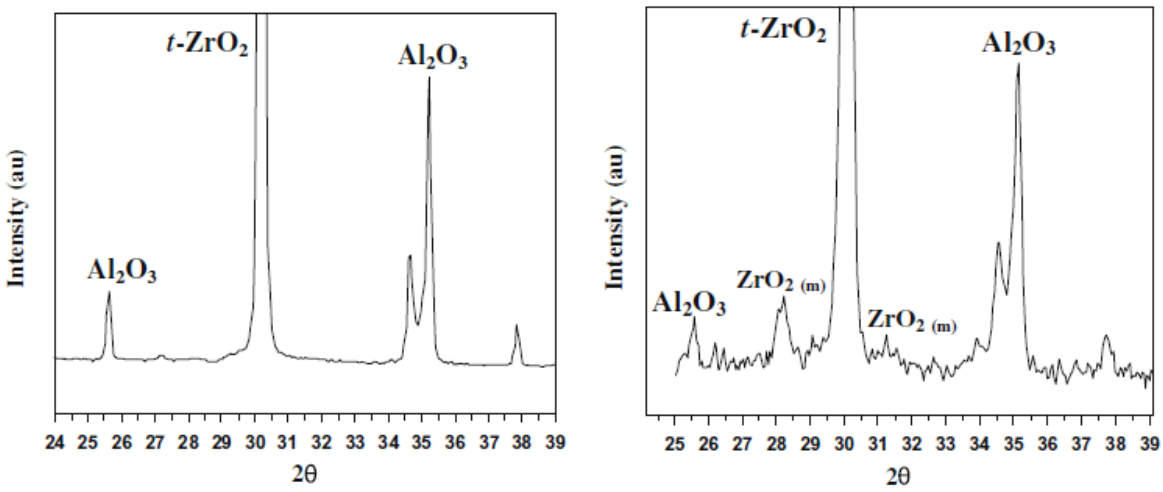

Fig. 8. XRD patterns of the (a) polished and (b) fracture surface of the pressureless sintered 30 wt.% Al_2O_3 (2.5 wt.% Al_2O_3 whiskers + 27.5 wt.% Al_2O_3 nanoparticles) + 70 wt.%TZ-3Y composites.

of ATZ ceramics [56]. It is speculated [45] that an increase in fracture toughness in the 30 wt.% Al_2O_3 (2.5 wt.% Al_2O_3 whiskers + 27.5 wt.% Al_2O_3 nanoparticles) + 70 wt.% TZ-3Y ceramic composite could be due to the increase in the amount of transformed monoclinic phase on the fracture surface of the specimen resulting from the induced stresses, owing to mismatch between thermal expansion coefficients of the ZrO_2 (TZ-3Y) matrix ($10.3x10^{-6}\,^oC^{-1}$) and Al_2O_3 ($8.1x10^{-6}\,^oC^{-1}$) grains or alternately to the formation of matrix microcracks prior to or during fracture of the ceramic composite (Fig. 7a). Fig. 8 shows the X-ray diffraction (XRD) patterns of the above composite, where the polished surface shows a phase composition of α-Al_2O_3 and tetragonal (*t*) zirconia phase (Fig. 8a), while the fracture surface (Fig. 8b) illustrates the presence of α-Al_2O_3, tetragonal (*t*) as well as monoclinic (*m*) zirconia phase. An increase in the presence of monoclinic (*m*) phase in the fracture surface due to the tetragonal (*t*) to monoclinic

(*m*) phase transformation during the fracture process is evident.

Conclusions

From the pressureless sintered $Al_2O_{3(w)} + Al_2O_{3(n)} + ZrO_2(TZ3Y)_n$ (90, 80 and 70 wt.%) composites investigated, the following can be concluded:

Relative densities between 75% and 97% were attained in the different composites. In all cases the grain size was maintained at a submicron scale at a processing temperature of 1500 ºC.

The 2.5 wt.% Al_2O_3 whiskers + 27.5 wt.% Al_2O_3 nanoparticles + 70 wt.% TZ-3Y composite showed a hardness > 13 GPa and a maximum fracture toughness of 6.9 MPa $m^{-1/2}$ with an average grain size of 0.4 ± 0.17 ım. The remaining porosity could contribute to obtaining a wide range of hardness as well as fracture toughness by varying the Al_2O_3 whiskers and the ZrO_2 (TZ-3Y) content, the homogeneous dispersion of whiskers being a challenge.

In the relative absence of whisker pull-out, it is suggested that the crack deflection mechanism was more efficient for ceramic composites with the addition of alumina whiskers compared with the whisker-free sample, where the fracture surface was relatively smooth with a decreasing of fracture toughness up to 28% with respect to alumina whisker toughening ceramics (AWTC).

An increase in fracture toughness in the 30 wt.% Al_2O_3 (2.5 wt.% Al_2O_3 whiskers + 27.5 wt.% Al_2O_3 nanoparticles) + 70 wt.% TZ3Y ceramic composite could be due to the increase in the amount of transformed monoclinic phase on the fracture surface of the specimen as result of the fracture process as well as to the residual stresses associated with differential coefficients of thermal expansion between the TZ-3Y matrix and the Al_2O_3 grains. An increase in the

presence of the monoclinic (*m*) phase in the fracture surface due to the tetragonal (*t*) to monoclinic (*m*) phase transformation during the fracture process could also contribute to explaining the increase in fracture toughness.

A wide range of final densities, grain sizes, Vickers hardness and fracture toughness can be obtained in AWTC by varying the Al_2O_3 whiskers and the ZrO_2 (TZ-3Y) content, which can be used to suit the composite ceramic properties to diverse dental applications.

References

[1] Daguano JKMF, Santos C, Souza RC, Balestra RM, Strecker K, Elias CN. Properties of ZrO2–Al2O3 composite as a function of isothermal holding time. Int J Ref Mat Hard Mat 2007;25:374–9.

[2] Guazzato M, Albakry M, Ringer SP, Swain MV. Strength, fracture toughness and microstructure of a selection of all-ceramic materials. Part II. Zirconia-based dental ceramics. Dental Mater 2004;20:449–56.

[3] Correa de Sá e Benavides de Morales MC, Carlos NE, Duailibi FJ, Gulmaraes de Oliveira L. Mechanical properties of alumina–zirconia composites for ceramic abutments. Mater Res 2004;7:643–9.

[4] Nikolay D, Kollenberg W, Deller K, Oswald M, Tontrup C. Manufacturing and properties of ZTA ceramics with nanoscaled ZrO2. Proc Eng 2006;4:E35–7.

[5] Leutbecher T, Hulsenberg D. Oxide fiber reinforced glass: a challenge to new composites. Adv Eng Mater 2000;3:93–9.

[6] Zhang X, Xu L, Du S, Han J, Hu P, Han W. Fabrication and mechanical properties of ZrB2–SiCw ceramic matrix composite. Mater Lett 2008;62:1058–60.

[7] Zhang X, Xu L, Du S, Han W, Han J. Crack-healing behavior of zirconium diboride composite reinforced with silicon carbide whiskers. Scr Mater 2008;59:1222–5.

[8] Zhang X, Xu L, Han W, Weng L, Han J, Du S. Mirostructure and properties of silicon carbide whisker reinforced diboride ultra-high temperature ceramics. Solid State Sci 2009;11:156–61.

[9] Lawn BR. Fracture of brittle solids. London: Cambridge University Press; 1993 [chapter 8].

[10] Xu HHK, Jahanmir S, Ives LK. Material removal and damage formation mechanisms in grinding silicon nitride. J

Mater Res 1996;11:1717–24.
[11] Iwanaga H, Kawai C. Tensile strength of silicon nitride whiskers synthesized by reaction amorphous silicon nitride and titanium dioxide. J Am Ceram Soc 1998;81:773–6.
[12] Xu HHK, Eichmiller FC, Antonucci JM, Schumacher GE, Ives LK. Dental resin composites containing ceramic whiskers and procured glass ionomer particles. Dent Mater 2000;16:356–63.
[13] Xu HHK, Ostertag CP, Braun LM, Lloyd IK. Short-crack mechanical properties and failure mechanisms of Si3N4-matrix/SiC-fiber composites. J Am Ceram Soc 1994;77:1889–96.
[14] Xu HHK, Martin TA, Antonucci JM, Eichmiller FC. Ceramic whisker reinforcement of dental resin composites. J Dent Res 1999;78:706–12.
[15] Becher PF, Wei GC. Toughening behavior in SiC-whisker-reinforced alumina. J Am Ceram Soc 1984;67:C267–9.
[16] Wei GC, Becher PF. Development of SiC-whisker-reinforced ceramics. Am Ceram Soc Bull 1985;64:289–304.
[17] Evans AG. High toughness ceramics. Mater Sci Eng 1998;A105(/106):65–75.
[18] Becher PF. Toughening behavior in ceramics associated with the deformation of tetragonal zirconia. Acta Metall 1986;34:1885–91.
[19] Hsueh CH. Some considerations of evaluation of interfacial frictional stress from the indentation technique for fibre-reinforced ceramic composites. J Mater Sci Lett 1989;8:739–42.
[20] Liu H, Weisskopf KL, Petzow G. Crack deflection process for hot-pressed whisker-reinforced ceramic composites. J Am Ceram Soc 1989;72:559–63.
[21] Faber KT, Evans AG. Crack deflection processes I. Theory. Acta Metall 1983;31:565–76.
[22] Carter DH, Hurley GF. Crack deflection as a toughening mechanism in SiCwhisker-reinforced MoSi2. J Am Ceram Soc 1987;70:C79–81.
[23] Singh JP, Goretta KC, Kupperrman DS, Routbort JL, Rhodes JF. Fracture oughness and strength of SiC-whisker-reinforced Si3N4 composites. Adv Ceram Mater 1988;3:357–60.
[24] Becher PF, Hsueh CH, Angelini P, Tiegs TN. Toughening behavior in whiskerreinforced ceramic matrix composites. J Am Ceram Soc 1988;71:1050–61.
[25] Ruhle M, Dalgleish BJ, Evans AG. On the toughening of ceramics by whiskers. Scr Met 1987;21:681–6.
[26] Kunz-Douglass S, Beaumont PWR, Ashby MF. A model for toughness of epoxyrubber particulate composites. J Mater

Sci 1980;15:1109–13.
[27] Krstic VD, Nicholson PS, Hoagland RG. Toughening of glasses by metallic particles. J Am Ceram Soc 1981;64:499–504.
[28] Rodel J, Fuller Jr ER, Lawn BR. In situ observations of toughening processes in alumina reinforced with silicon carbide whiskers. J Am Ceram Soc 1991;74:3154–7.
[29] Chevalier J. What future for zirconia as a biomaterial? Biomaterials 2006;27:535–43.
[30] De Aza AH, Chevalier J, Fantozzi G. Crack growth resistance of alumina, zirconia and zirconia toughened alumina ceramics for joint prostheses. Biomaterials 2002;23:937–45.
[31] Ruhle M, Stecker A, Waidelich D, Kraus B. In situ observations of stressinduced phase transformation in ZrO2 containing ceramics. In: Claussen N, Rulle M, Heuer A, editors. Advanced in ceramics. Science and Technology II. Columbus: American Ceramic Society; 1984.
[32] Gregori G, Burger W, Sergo V. Piezo-spectroscopic analysis of the residual stress in zirconia-toughened alumina ceramics: the influence of the tetragonal-to-monoclinic transformation. Mater Sci Eng 1999;A271:401–6
[33] Guazzato M, Albakry M, Ringer SP, Swain MV. Strength, fracture toughness and microestructure of a selection of all-ceramic materials. Part I. Pressable and alumina glass-infiltrated ceramics. Dent Mater 2004;20:441–8.
[34] Evans AG. Perspective on the development of high-toughness ceramics. J Am Ceram Soc 1990;73:187–206.
[35] Sjolin R, Sundh A, Bergman M. The decim system for the production of dental restorations. Int J Comput Dent 1999;2:197–207.

[36] Christel P, Meunier A, Heller M, Torre JP, Peille CN. Mechanical properties and short-term in-vivo evaluation of yttrium-oxide partially-stabilized zirconia. J Biomed Mater Res 1989;23:45–61.
[37] Hannink RH, Kelly PM, Muddle BC. Transformation toughening in zirconiacontaining ceramics. J Am Ceram Soc 2000;83:461–87.
[38] Gutknecht D, Chevalier J, Garnier V, Fantozzi G. Key role of processing to avoid low temperature ageinig in alumina zirconia composites for orthopedic application. J Eur Ceram Soc 2007;27:1547–52.
[39] Anusavice J. Clasificación de los materiales de reconstrucción dental (Classification of materials used in dental reconstruction). Phillips‘ Science of Dental Materials 11º edición, Kennet Elsevier España, SA Génova; 2004.
[40] Nelly JR, Denry I. Stabilized zirconia as structural ceramic: an overview. Dent Mater 2008;24:289–98.
[41] Duszova A, Dusza J, Tomasek K, Blugan G, Kuebler J. Microstructure and properties of carbon/nanotube zirconia composite. J Eur Ceram Soc 2008;28: 1023–7.
[42] Ponton CB, Rawlings RD. Dependence of the Vickers indentation fracture toughness on the surface crack length. Br Ceram Trans J 1989;88:83–90.
[43] ASTM C-1327–99. Standard test method for Vickers indentation hardness of advanced ceramics. Annual Book of ASTM Standards, vol. 14.02; 1999.
[44] Evans AG, Charles EA. Fracture toughness determinations by indentation. J Am Ceram Soc 1976;59:371–2.
[45] Microstructure and properties of alumina-whisker-reinforced tetragonal polycrystal matrix composites. CONF910162–1; 1991.
[46] Bengisu M, Inal OT. Whisker toughening of ceramics: toughening mechanisms, fabrication and composite properties. Annu Rev Mater Sci 1994;24:83–124.
[47] Yang M, Stevens R. Microstructure and properties of SiC whisker reinforced ceramic composites. J Mater Sci 1991;26:726–36.
[48] Bjork J, Hermansson LAG. Hot isostatically pressed alumina-silicon carbidewhisker composite. J Am Ceram Soc 1989;72:1436–8.
[49] Tekeli S. Fracture toughness (*K*IC), hardness, sintering and grain growth behaviour of 8YSCZ/Al2O3 composites

produced by colloidal processing. J Alloys Compd 2005;391:217–24.

[50] Wook An J, Soon Lim Dae. Effect of carbon nanotube additions on the microstructure of hot-pressed alumina. J Ceram Proc Res 2002;3:201–4.

[51] Suzuki HY, Shinosaki K, Kuroi H, Tashima S. Sintered microstructure and mechanical properties of high purity alumina ceramics made by high-speed centrifugal compaction process. Key Eng Mater 1999;159–160:187–92.

[52] Chakravarty D, Bysakh S, Muraleedhran K, Narasigna Rao T, Sundaresan R. Spark plasma sintering of magnesia-doped alumina with high hardness and fracture toughness. J Am Ceram Soc 2008;91:203–8.

[53] Zhang Y, Chen J, Hu L, Liu W. Presureless-sintering behavior of nanocrystalline ZrO2–Y2O3–Al2O3 system. Mater Lett 2006;60:2302–5.

[54] Thompson JI, Anusavice KJ, Balasubramaniam B, Mecholsky JJ. Effect of microcraking on the fracture toughness and fracture surface fractal dimension of Lithia-based glass-ceramics. J Am Ceram Soc 1995;78:3045–9.

[55] Celli A, Tucci A, Esposito L. Quatitative evaluation by fractal analysis of indentation crack paths in Si3N4–SiCw composites. J Eur Ceram Soc 1999;19:441–9.

[56] Wang X, Tian J, Yu X, Shan Y, Liu Z, Yin Y. Effect of microstructure on the fracture behavior of micro-nano ZTA composite. Mater Chem Phys 2008;112:213–7.